CrossMark

ORIGINAL ARTICLE

Influence of the GLONASS inter-frequency bias on differential code bias estimation and ionospheric modeling

Xiaohong Zhang[1,2] · Weiliang Xie[1] · Xiaodong Ren[1] · Xingxing Li[3] · Keke Zhang[1] · Weiping Jiang[4]

Abstract Due to the application of frequency division multiple access, the signals of GLONASS satellites suffer from code and carrier phase inter-frequency biases (IFBs). In this study, the effects of GLONASS code IFBs on differential code bias (DCB) estimation and ionospheric modeling are investigated. The observational data from more than 130 MGEX stations for a period of 60 days are used to generate the DCB products, with and without considering the GLONASS code IFB. According to the results, residuals of the DCB estimation without GLONASS code IFB consideration exhibit frequency-dependent systematic errors, errors that can be eliminated when the GLONASS code IFB is taken into account. The GLONASS inter-frequency differential code bias (IFDCB), defined as the difference of the sum of satellite and receiver DCB estimates without and with GLONASS code IFB consideration, is taken to represent the difference between the two DCB estimation types. The IFDCBs are generally in the range of ± 4 and ± 2 ns for C1P–C2P and C1C–C1P, respectively, and the largest difference of the C1P–C2P IFDCBs between frequency channels is >7 ns. The VTEC products of ionospheric modeling with and without the consideration of the GLONASS code IFB are also

generated based on data from 30 days of MGEX and IGS networks. The mean difference and standard deviation between them are 0.53–1.13 and 0.98–1.75 TECU, respectively.

Keywords GLONASS · Inter-frequency bias (IFB) · Differential code bias (DCB) · Ionospheric modeling · MGEX

Introduction

Due to frequency division multiple access (FDMA) technology (ICD-GLONASS 2008), GLONASS signals suffer from different code and phase delays in the receiving equipment, which leads to difficulties in GPS/GLONASS combined precise point positioning (PPP) (Li et al. 2015) and relative positioning (Yamada et al. 2010). Previous studies have demonstrated that the carrier phase inter-frequency bias (IFB) of GLONASS satellites are linear functions of the frequency (Pratt et al. 1998; Al-Shaery et al. 2013; Wanninger 2012), but seems to be difficult to model. Some studies have noted that the GLONASS code IFB could be as much as several meters (Tsujii et al. 2000). Kozlov et al. (2000) showed that the GLONASS code IFBs tend to be characteristic for receivers of a certain type and are relatively stable. Shi et al. (2013) used data from 133 stations of five manufacturers to analyze the characteristics of the GLONASS code IFB. They found that the ionospheric-free combinations of the GLONASS code IFB showed strong correlations for receivers with the same firmware and that the precision of PPP after code IFB calibration was greatly improved during the convergence period.

✉ Xiaodong Ren
xdren@whu.edu.cn

1 School of Geodesy and Geomatics, Wuhan University, 129 Luoyu Road, Wuhan 430079, Hubei, China

2 Collaborative Innovation Center for Geospatial Technology, 129 Luoyu Road, Wuhan 430079, Hubei, China

3 German Research Centre for Geosciences (GFZ), Telegrafenberg, 14473 Potsdam, Germany

4 GPS Research Center, Wuhan University, 129 Luoyu Road, Wuhan 430079, Hubei, China

Generally, differential code bias (DCB), which includes the intra- and inter-frequency difference of pseudorange hardware delays, should be precisely determined in ionospheric modeling (Lanyi and Roth 1988; Wilson and Mannucci 1993; Conte et al. 2011) and precise positioning (Øvstedal 2002; Wielgosz 2011; Li et al. 2013). In order to provide DCB and global ionospheric map (GIM) products, an ionospheric working group was established by the International GNSS Service (IGS) in 1998 (Feltens 2003; Hernández-Pajares et al. 2009). It consists of four Ionospheric Associate Analysis Centers (IAACs), including the Center for Orbit Determination in Europe (CODE), Jet Propulsion Laboratory (JPL), European Space Agency (ESA), and Polytechnic University of Catalonia (UPC). CODE is the only IAAC that is capable of providing the GPS + GLONASS DCB and GIM products. The products of the other IAACs are generated using different approaches based on GPS-only observations (Mannucci et al. 1998; Hernández-Pajares et al. 1999; Schaer 1999; Feltens 2007). With the modernization of GPS and GLONASS as well as the rapid development of the BeiDou and Galileo systems, many groups are investigating the methods of multi-GNSS DCB determination and ionospheric modeling (Wang et al. 2015; Ren et al. 2016). However, only one receiver DCB parameter per satellite system was estimated in the existing studies (Hauschild and Montenbruck 2016). This limitation shows no effect on the DCB estimation for GPS, BeiDou, and Galileo, but it matters in the case of GLONASS. Due to the existence of code IFBs, the receiver DCBs of GLONASS differs for satellites on different frequency channels. Therefore, setting the receiver DCB as one parameter is insufficient for GLONASS. Until recently, few researchers have analyzed the influence of the GLONASS code IFB on DCB estimation and ionospheric modeling. A detailed investigation on the characteristics of the GLONASS code IFB is crucial for GLONASS-related ionospheric modeling and DCB estimation.

We propose an improved method for DCB estimation and ionospheric modeling when considering the GLONASS code IFB in following aspects: First, the GPS and GLONASS DCBs are estimated without considering the GLONASS code IFB, which are then compared with DCB products from CODE, German Aerospace Center (DLR), and Institute of Geodesy and Geophysics (IGG). Second, the distribution of residuals is analyzed to investigate their correlation with the frequency channel. After that, GLONASS DCBs with code IFB consideration are generated, and the corresponding residuals are analyzed. According to the analysis, the difference between the DCBs estimated with and without GLONASS code IFB consideration are derived and investigated. Finally, the GIMs obtained with and without GLONASS code IFB consideration are compared with each other to investigate the influence of IFB on ionospheric modeling.

Methods

There are many different methods for DCB estimation and ionospheric modeling, but few of them have taken the GLONASS code IFB into account. In this section, we first describe the most commonly used methods of DCB estimation and ionospheric modeling with no consideration of the GLONASS code IFB and then propose an improved method that considers the GLONASS code IFB.

DCB estimation and ionospheric modeling without GLONASS code IFB consideration

Ignoring the effects of multipath and noise, the pseudorange observation equations for GPS and GLONASS can be described as follows:

$$
\begin{cases}
P_1^{\text{sys},i} = \rho_r^i + I_{r,1}^i + T_r^i + c \cdot (dt_r - dt^i) + b_{r,1}^{\text{sys}} + b_1^{\text{sys},i} \\
P_2^{\text{sys},i} = \rho_r^i + I_{r,2}^i + T_r^i + c \cdot (dt_r - dt^i) + b_{r,2}^{\text{sys}} + b_2^{\text{sys},i}
\end{cases}
$$

(1)

where the superscript sys represents the GPS or GLONASS system. The superscript i and subscript r refer to satellite and station, respectively, $P_1^{\text{sys},i}$ and $P_2^{\text{sys},i}$ are the pseudorange observations at frequency f_1 and f_2, respectively, ρ_r^i is the geometric distance from satellite i to station r, $I_{r,1}^i$ and $I_{r,2}^i$ are the ionospheric delays at frequency f_1 and f_2 respectively, T_r^i is the tropospheric delay, c is the speed of light in vacuum, dt^i and dt_r express the satellite and receiver clock biases, respectively, and b^i and b_r stand for satellite and receiver hardware delay of pseudorange, respectively. Utilizing the difference in the pseudorange observations between two given frequencies, the geometry-free combination can be obtained as follows:

$$
\begin{cases}
P_4^{G,i} = P_1^{G,i} - P_2^{G,i} = 40.31 \cdot \left(\dfrac{1}{f_{G,1}^2} - \dfrac{1}{f_{G,2}^2} \right) \cdot \text{STEC}_r^{G,i} + \text{DCB}_r^G + \text{DCB}^{G,i} \\
P_4^{R,j} = P_1^{R,j} - P_2^{R,j} = 40.31 \cdot \left(\dfrac{1}{f_{j,1}^2} - \dfrac{1}{f_{j,2}^2} \right) \cdot \text{STEC}_r^{R,j} + \text{DCB}_r^R + \text{DCB}^{R,j}
\end{cases}
$$

(2)

where STEC_r^i represents the slant total electron content (STEC) along the signal propagation path from satellite i to station r, ignoring the higher-order contributions, $f_{G,1}$ and $f_{G,2}$ are the frequencies of the GPS at carrier phases L_1 and L_2, respectively, $f_{j,1}$ and $f_{j,2}$ are the frequencies of the GLONASS satellite j at carrier phases L_1 and L_2, respectively, $\text{DCB}_r^G = b_{r,1}^G - b_{r,2}^G$ and $\text{DCB}^{G,i} = b_1^{G,i} - b_2^{G,i}$ are

the receiver and satellite DCBs of GPS, respectively, and $\text{DCB}_r^R = b_{r,1}^R - b_{r,2}^R$ and $\text{DCB}^{R,j} = b_1^{R,j} - b_2^{R,j}$ refer to the receiver and satellite DCBs of GLONASS, respectively. Owing to the different frequencies and signal structures of the individual GNSSs, DCB_r^G and DCB_r^R are different for the same receiver. When the GLONASS code IFB is not considered, the receiver DCB is generally regarded to be equal for all satellites in each system.

Equation (2) in which the pseudorange observations are smoothed by carrier phase has usually been used to estimate the GIM and DCB products by the IAACs. Because of the pseudorange measurement noise, the precision of the carrier phase is much higher than that of the pseudorange. However, an ambiguity parameter from the carrier phase measurement must be considered. In order to achieve a trade-off between precision and complexity, the "leveling carrier to code" algorithm is applied by many ionospheric researchers (Ciraolo et al. 2007). The ionospheric observations of GPS and GLONASS can be described as:

$$\begin{cases} \hat{P}_4^{G,i} = 40.31 \cdot \left(\dfrac{1}{f_{G,1}^2} - \dfrac{1}{f_{G,2}^2} \right) \cdot \text{STEC}_r^{G,i} + \text{DCB}_r^G + \text{DCB}^{G,i} \\ \hat{P}_4^{R,j} = 40.31 \cdot \left(\dfrac{1}{f_{j,1}^2} - \dfrac{1}{f_{j,2}^2} \right) \cdot \text{STEC}_r^{R,j} + \text{DCB}_r^R + \text{DCB}^{R,j} \end{cases}$$

$$(3)$$

where $\hat{P}_4^{G,i}$ and $\hat{P}_4^{R,j}$ are phase-smoothed pseudorange observations. The other parameters in (3) were defined in (2).

There are many well-established methods for modeling the spatial distribution of the vertical total electron content (VTEC). The spherical harmonic expansion model is widely used in global ionospheric modeling due to its accuracy and simplicity:

$$\text{VTEC}(\varphi, \lambda) = \sum_{n=0}^{N} \sum_{m=0}^{n} \tilde{P}_{nm}(\sin \varphi) \left(\tilde{C}_{nm} \cos(m\lambda) + \tilde{S}_{nm} \sin(m\lambda) \right)$$

$$\text{STEC}(\varphi, \lambda) = \text{VTEC}(\varphi, \lambda) \cdot M(z) \qquad (4)$$

$$M(z) = \frac{1}{\cos z'}, \quad \sin z' = \frac{R}{R+H} \sin z$$

where φ and λ are the geomagnetic latitude and solar-fixed longitude of the ionospheric pierce point (IPP), respectively, $\text{VTEC}(\varphi, \lambda)$ denotes the vertical ionospheric TEC at the IPP (φ, λ), N is the max degree of the spherical function, $\tilde{P}_{nm}$ represents a regularization Legendre series of degree n and order m, $\tilde{C}_{nm}$ and $\tilde{S}_{nm}$ are spherical harmonic coefficients to be estimated, $M(z)$ is the mapping function, which is used to convert STEC to VTEC, R is the mean radius of the earth, $H = 450 \, \text{km}$ is the altitude of the single-layer ionosphere, z is satellite zenith angle at the receiver, and z' is satellite zenith angle at the corresponding IPP.

When all of the observations of GPS and GLONASS are combined, Eq. (3) is singular. To separate the satellite and receiver DCBs, the zero-mean condition for satellite DCBs is usually adopted, which can be expressed as (Li et al. 2012):

$$\begin{cases} \sum\limits_{i=1}^{N_G} \text{DCB}^{G,i} = 0 \\ \sum\limits_{j=1}^{N_R} \text{DCB}^{R,j} = 0 \end{cases} \qquad (5)$$

where N_G and N_R refer to the number of GPS and GLONASS satellites, respectively. Thus, the GIM and DCBs can be determined. The estimated parameters are,

$$X = \left(\tilde{C}_{nm} \tilde{S}_{nm} \text{DCB}^{G,i} \text{DCB}_r^G \text{DCB}^{R,j} \text{DCB}_r^R \right)^{\text{T}} \qquad (6)$$

In order to simplify the process of DCB estimation, many researchers estimate the DCB after eliminating ionospheric delays using an existing GIM. The DCBs of satellites and receivers are generally regarded as constant throughout a single day, and the multipath and noise are assumed to have a zero-mean average over a one-day period (Montenbruck et al. 2014). In addition, a cutoff elevation of 20° is applied to reduce the ionospheric modeling errors. The satellite plus receiver DCB (SPRDCB) can be obtained as follows:

$$\begin{cases} \text{DCB}_r^G + \text{DCB}^{G,i} = \dfrac{1}{N_r^i} \sum\limits_{k=1}^{N_r^i} \left[P_4^{G,i} - 40.31 \cdot \left(\dfrac{1}{f_{G,1}^2} - \dfrac{1}{f_{G,2}^2} \right) \cdot \text{VTEC}_r^i \cdot M(z_r^i) \right] \\ \text{DCB}_r^R + \text{DCB}^{R,j} = \dfrac{1}{N_r^j} \sum\limits_{k=1}^{N_r^j} \left[P_4^{R,j} - 40.31 \cdot \left(\dfrac{1}{f_{j,1}^2} - \dfrac{1}{f_{j,2}^2} \right) \cdot \text{VTEC}_r^j \cdot M(z_r^j) \right] \end{cases}$$

$$(7)$$

where N_r^i and N_r^j are the number of epochs that station r tracks GPS satellite i and GLONASS satellite j, respectively, over a day. By repeating the above procedures station by station, the SPRDCB of all satellites and sites can be obtained. The estimated parameters are:

$$X = \left(\text{DCB}^{G,i} \text{DCB}_r^G \text{DCB}^{R,j} \text{DCB}_r^R \right)^T \qquad (8)$$

The condition Eq. (5) should also be imposed to separate the DCBs of satellites and receivers. Thus, the receiver and satellite DCBs for GPS and GLONASS without GLONASS code IFB consideration can be obtained.

An improved method for DCB estimation and ionospheric modeling with GLONASS code IFB consideration

In DCB estimation and ionospheric modeling without GLONASS code IFB consideration, only one receiver DCB parameter for GLONASS is estimated at each station. Since the GLONASS satellites emit signals on individual frequencies, the receiver DCB depends on the satellite

frequency channel. We propose an improved DCB estimation and ionospheric modeling method by considering the GLONASS code IFB. Assuming that the receiver DCBs of GLONASS satellites of different frequencies are not equal, we set one receiver DCB parameter per GLONASS frequency channel at each station.

Considering the GLONASS code IFB, the SPRDCB can be expressed as follows:

$$
\mathrm{DCB}_r^{R,f} + \mathrm{DCB}^{R,j} = \frac{1}{N_r^j} \sum_{i=1}^{N_r^j}
$$

$$
\times \left[P_4^{R,j} - 40.31 \cdot \left(\frac{1}{f_{j,1}^2} - \frac{1}{f_{j,2}^2} \right) \cdot \mathrm{VTEC}_r^j \cdot M(z_r^j) \right] \tag{9}
$$

where $\mathrm{DCB}_r^{R,f}$ refers to the receiver DCB of station r and GLONASS frequency channel number f. Unlike with DCB estimation without GLONASS code IFB consideration, there is a receiver DCB parameter per frequency channel for GLONASS at each station.

When all observations are integrated, the rank deficiency is equal to the number of frequency channels of GLONASS. We constrain the sum of the receiver DCBs of all stations for each GLONASS frequency to zero, which can be expressed as follows:

$$
\begin{cases}
\mathrm{DCB}_1^{R,f_1} + \mathrm{DCB}_2^{R,f_1} + \mathrm{DCB}_3^{R,f_1} + \cdots + \mathrm{DCB}_n^{R,f_1} = 0 \\
\mathrm{DCB}_1^{R,f_2} + \mathrm{DCB}_2^{R,f_2} + \mathrm{DCB}_3^{R,f_2} + \cdots + \mathrm{DCB}_n^{R,f_2} = 0 \\
\qquad\qquad\qquad\qquad \vdots \\
\mathrm{DCB}_1^{R,f_k} + \mathrm{DCB}_2^{R,f_k} + \mathrm{DCB}_3^{R,f_k} + \cdots + \mathrm{DCB}_n^{R,f_k} = 0
\end{cases} \tag{10}
$$

where $f_1, f_2 \ldots, f_k$ are the GLONASS frequency channels. Due to the introduction of the constraint Eq. (10), the estimated satellite and receiver DCBs are dependent on the stations selected. In this approach, the estimated parameters are:

$$
X = \left(\mathrm{DCB}^{R,j} \mathrm{DCB}_r^{R,f} \right)^{\mathrm{T}} \tag{11}
$$

Compared to the DCB estimation without GLONASS code IFB consideration, not only the common parts of receiver DCB for all satellites can be estimated but also the differences can be determined when the DCB is estimated considering GLONASS code IFB. In order to investigate the influence of the GLONASS code IFB on DCB estimation, DCB estimation differences with and without GLONASS code IFB consideration should be obtained. The difference is designated as inter-frequency differential code bias (IFDCB). The different condition Eqs. (5) and (10) are adopted for DCB estimation with and without GLONASS code IFB consideration, respectively. Thus, the IFDCB cannot be obtained by differencing the satellite or receiver DCB estimates because these belong to different datums. The condition equations are used to separate satellite and receiver DCBs, but they only show slight effects on the sum of satellite and receiver DCB estimations. Therefore, the IFDCB can be computed by subtracting the sum of satellite and receiver DCB estimations without GLONASS code IFB consideration from the sum of satellite and receiver DCB estimations with GLONASS code IFB consideration, which can be described as:

$$
\mathrm{IFDCB}_r^f = \mathrm{DCB}_r^{R,f}(c) + \mathrm{DCB}^{R,j}(c) - \mathrm{DCB}^{R,j}(n)
$$

$$
- \mathrm{DCB}_r^R(n) \tag{12}
$$

where IFDCB_r^f is the IFDCB of receiver r and frequency channel f. There are two GLONASS satellites for some frequency channels. Since each satellite can calculate an IFDCB from (12), the IFDCB_r^f represents the mean of two satellite IFDCBs. $\mathrm{DCB}_r^{R,f}(c)$ and $\mathrm{DCB}^{R,j}(c)$ refer to receiver and satellite DCB estimations with GLONASS code IFB consideration obtained by (9), and $\mathrm{DCB}^{R,j}(n)$ and $\mathrm{DCB}_r^R(n)$ refer to satellite and receiver DCB estimations without GLONASS code IFB consideration obtained by (7).

Similar to the DCB estimation, the ionospheric observation equations with GLONASS code IFB consideration can be expressed as:

$$
\begin{cases}
\hat{P}_4^{G,i} = 40.31 \cdot \left(\frac{1}{f_{G,1}^2} - \frac{1}{f_{G,2}^2} \right) \cdot \mathrm{STEC}_r^{G,i} + \mathrm{DCB}_r^G + \mathrm{DCB}^{G,i} \\
\hat{P}_4^{R,j} = 40.31 \cdot \left(\frac{1}{f_{j,1}^2} - \frac{1}{f_{j,2}^2} \right) \cdot \mathrm{STEC}_r^{R,j} + \mathrm{DCB}_r^{R,f} + \mathrm{DCB}^{R,j}
\end{cases} \tag{13}
$$

Equation (4) is used to model the STEC. The max degree of spherical harmonics is chosen as 15. In the time domain, a day is divided into 12 sessions with a 2-h interval, and the piecewise linear function is used to establish connections between GIMs from different sessions. Since the DCB can be considered to be constant throughout a single day, all observations from the various 2-h sessions in one day are processed in a common parameter adjustment procedure. For 400 stations and 14 GLONASS frequency channels, estimating the receiver DCBs of GLONASS for each station will introduce more than 4000 additional parameters, which is even more than the sum of all of the estimated ionospheric parameters (for the expansion of spherical harmonics up to a degree of 15 with a 2-h interval, there are $16 \times 16 \times 13$ ionospheric parameters). Li et al. (2015) proposed an ionospheric modeling method which used the pre-estimated products to remove the DCB in ionospheric observable, thus only ionospheric parameters need to be estimated. In consideration of computational efficiency, the satellite and receiver DCBs of GPS and GLONASS are

corrected by the DCB products estimated in (9). Thus, the estimated parameters are expressed as,

$$X = \left(\tilde{C}_{nm}\tilde{S}_{nm}\right)^{\mathrm{T}} \tag{14}$$

In this approach, only the spherical harmonic coefficients are in need of estimation, which provides great benefit for retrieving an accurate ionospheric model with high calculation efficiency.

Data collection and processing strategy

In this section, the influence of the GLONASS code IFB on DCB estimation and ionospheric modeling is investigated based on data from globally distributed IGS and MGEX network stations. The distribution of stations involved is described, and the data processing strategy is presented.

Data collection

Observations from over 130 MGEX stations for 60 days from January 1 to February 29, 2016, corresponding to DOY 1–60, have been used to estimate the DCBs of GLONASS, as well as the DCBs of GPS for comparison. Observations provided by these globally distributed MGEX stations are sufficient to retrieve the DCB, but they are insufficient for ionospheric modeling due to the sparse distribution of these stations. Thus, more than 400 stations from the IGS and MGEX networks are additionally introduced to construct the global ionospheric model. The distribution of contributing MGEX and IGS stations is shown in Fig. 1.

Processing strategy

In the RINEX 3 standard, there are many types of code observations with which to form the corresponding DCBs. In this study, we only focus on the commonly used DCBs, including C1C–C1W and C1W–C2W DCBs of GPS, as well as C1C–C1P and C1P–C2P DCBs of GLONASS. As mentioned previously, the DCB parameters can be

estimated as part of ionospheric modeling and estimation or after eliminating the ionospheric path delays first using an existing GIM. However, too many unknown parameters will need to be considered if the DCB parameters considering the GLONASS code IFB are estimated in the process of ionospheric modeling. Having computational efficiency and simplicity in mind, we estimate the DCB parameters with and without GLONASS code IFB consideration after eliminating the ionospheric path delays using an existing GIM. Since the errors in correcting the ionospheric path delay with the existing GIM are very large at low elevations, a cutoff elevation of 20° is applied.

For ionospheric modeling without GLONASS code IFB consideration, we estimate the DCB along with ionospheric parameters based on GPS + GLONASS observations collected by the IGS and MGEX networks. To reduce the multipath effects and noise level of the ionospheric measurements, carrier phase-smoothed code observations are used with an elevation mask of 10°. The same observations and corresponding processing strategy are also adopted for ionospheric modeling with GLONASS code IFB consideration. In order to reduce the number of unknown parameters in ionospheric modeling with considering GLONASS code IFB, the DCB parameters obtained from the DCB estimation with GLONASS code IFB consideration are introduced as known values.

Results and analysis

We analyze the influence of the GLONASS code IFB on DCB estimation and ionospheric modeling in detail. In order to investigate the performance of the traditional DCB estimation method and validate our ionosphere and DCB software "GIMP," we first derive the DCBs without GLONASS code IFB consideration are using (7). The DCB estimates generated using the "GIMP" software at the School of Geodesy and Geomatics (SGG) of Wuhan University are compared and validated with data provided by CODE, DLR, and IGG.

Validation of DCB estimations without GLONASS code IFB consideration

Figure 2 shows the differences of monthly GPS C1C–C1W and GLONASS C1C–C1P DCB products of SGG, DLR, and IGG with respect to CODE in January 2016. The satellites are labeled by their pseudorandom noise (PRN) number to avoid confusion. It can be seen that the monthly C1C–C1W DCB of SGG, DLR, and IGG reveals good agreement with those of CODE. The differences are mainly within ±0.1 ns, and the largest difference is
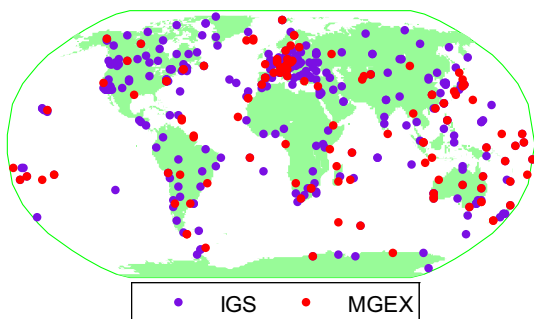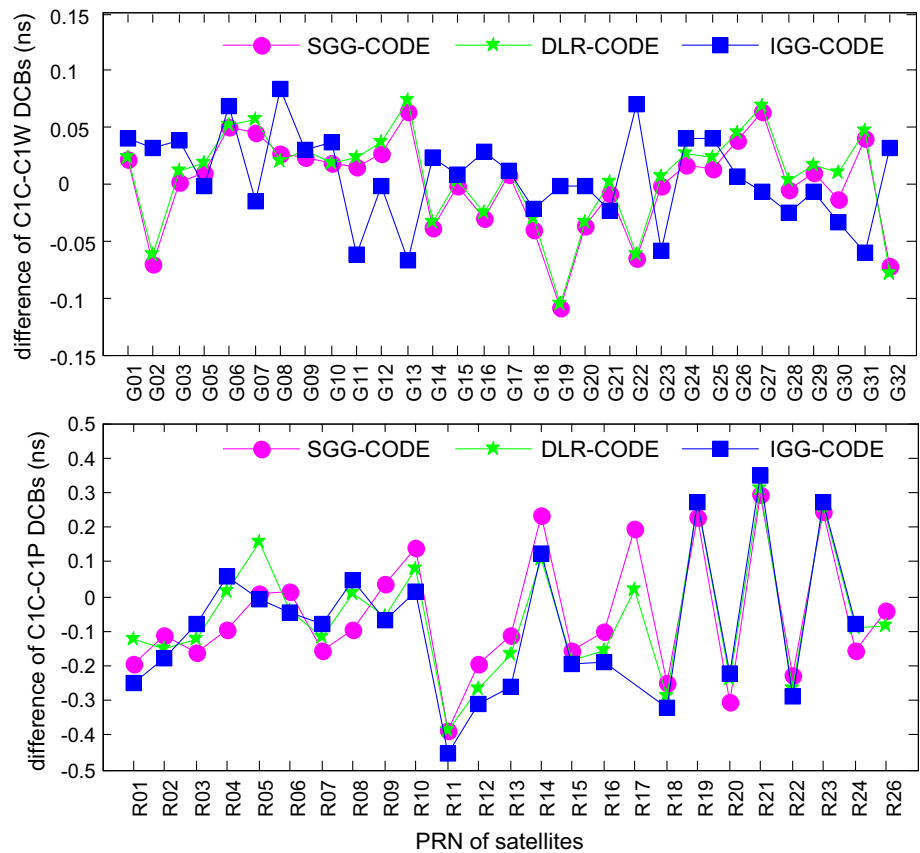

**Fig. 1** Distribution of contributing MGEX and IGS stations

0.109 ns for G19 (−0.109, −0.105, and −0.002 ns for SGG, DLR, and IGG, respectively). The differences for GLONASS C1C–C1P DCBs are slightly larger than those for GPS C1C–C1W DCBs, but are generally less than ±0.5 ns, with the largest differences of approximately 0.45 ns for R11 (−0.39, −0.39 and 0.45 ns for SGG, DLR, and IGG, respectively). Wang et al. (2015) assessed the performance of these types of DCBs based on MGEX data for December 2014 and found similar characteristics. They reported that the largest difference of GPS C1C–C1W DCBs between CODE and DLR/IGG was approximately 0.6 ns and that the GLONASS C1C–C1P DCB errors relative to CODE were higher than those of the GPS C1C–C1W DCBs (approximately 0.1 ns). According to our result as well as the comparison with data presented in Wang et al. (2015), it is demonstrated that the DCB products of the GPS C1C–C1W, and GLONASS C1C–C1P retrieved from the "GIMP" software are of sufficient accuracy and quality.

The GPS C1W–C2W and GLONASS C1P–C2P DCB products of CODE, corresponding to the P1–P2 DCBs in IONEX format provided in the daily GIM product, are introduced as references to validate the DCBs of SGG. The mean difference and standard deviation (STD) of SGG/DLR/IGG for each satellite from DOY 1 to 60 for 2016 are

presented in Fig. 3. It is seen that the GPS C1W–C2W DCB of SGG, DLR, and IGG shows good agreement with the CODE and the mean differences are within ±0.5 ns. Moreover, the C1W–C2W DCBs of SGG and DLR show better consistency with CODE than IGG, since the STD of SGG and DLR is smaller than that of IGG. It is noteworthy that the C1W–C2W DCB of G04 is absent for IGG because this satellite can only be tracked <10 days during this period. The mean differences of the GLONASS C1P–C2P DCBs vary between −1.5 and 1 ns for all satellites, which are slightly larger than those of the GPS C1W–C2W DCBs, whereas the differences of the DCBs of SGG, DLR, and IGG are almost the same. The larger difference of the C1P–C2P DCBs between SGG/DLR/IGG and CODE may be the result of using observational data from different networks, since the DCB products of SGG/DLR/IGG are generated based on the MGEX network and the CODE DCB products are based on the IGS network. It can also be observed that R17 and R26 show larger differences than other satellites. This could be because the CODE DCB products for the two satellites display jumps more frequently than the SGG, DLR, and IGG data during this period. Although there are some differences in the DCB products between SGG/DLR/IGG and CODE, they are generally in good agreement with each other.

Fig. 3 Mean difference and STD of the GPS C1W–C2W and GLONASS C1P–C2P DCB estimates with respect to CODE for the period DOY 1–60 in 2016. *Dots* denote the mean differences of SGG, DLR, and IGG of the corresponding satellite, and the lengths of the *vertical lines* represent their respective STDs
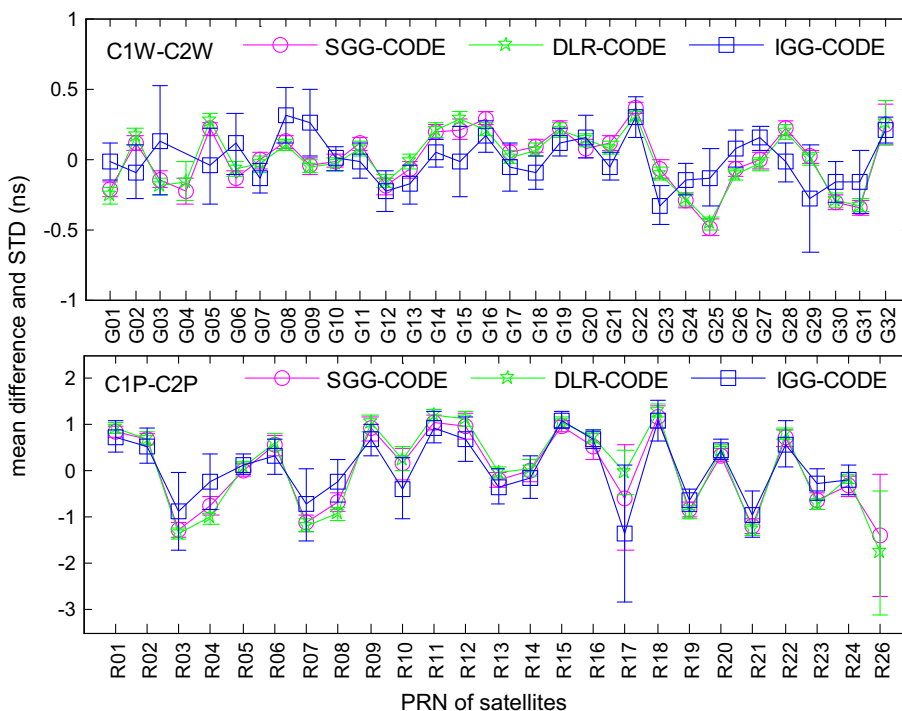
Analysis of the residuals of DCB estimation without GLONASS code IFB consideration

In order to further assess the performance of the current DCB estimation, the residual distributions of the GPS C1C–C1W and C1W–C2W as well as of GLONASS C1C–C1P and C1P–C2P SPRDCBs for all contributing stations from DOY 1 to 60 in 2016 are presented in Fig. 4. The residual distributions of the GPS C1C–C1W and C1W–C2W SPRDCBs show a zero-mean normal distribution, and the residuals of the latter are more scattered than those of the former, with STDs of 0.04 and 0.16 ns for C1C–C1W and C1W–C2W, respectively. The residuals of the GLONASS C1C–C1P and C1P–C2P SPRDCBs also follow a zero-mean normal distribution, but are slightly asymmetric, and the STD of latter is also larger than that of the former (approximately 0.19 and 0.43 ns for C1C–C1P and C1P–C2P, respectively). Two important observations can be obtained from the aforementioned analysis: (1) The residual distribution of the SPRDCBs on different frequencies is more scattered than that of SPRDCBs on a common frequency in each satellite system. (2) The STDs of the residuals of the GLONASS SPRDCBs are larger than those of the GPS SPRDCBs on the same or different frequencies. The reason for the first observation could be that DCBs on different frequencies are calculated based on IGS GIM products, while DCBs on the same frequency do not need the IGS GIM products. The second observation has also been reported by Wang et al. (2015). They found that the residuals of SPRDCBs of GLONASS were more
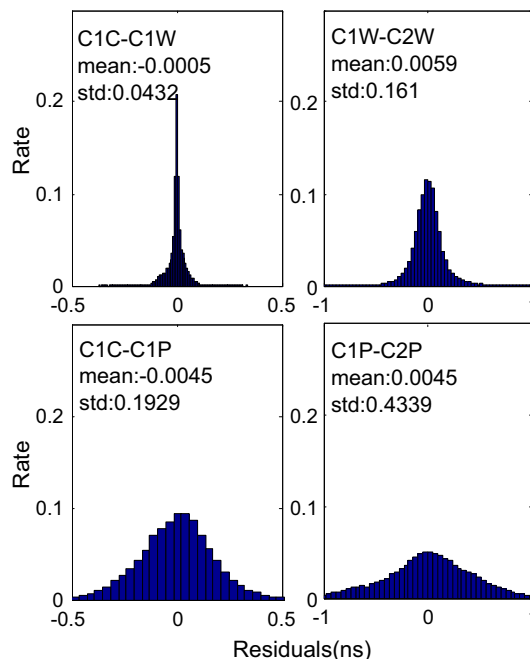

Fig. 4 Residual distribution of GPS C1C–C1W, C1W–C2W, GLONASS C1C–C1P, and C1P–C2P SPRDCBs obtained by DCB estimation without GLONASS code IFB consideration, overlaid with normal probability density function curves (*in red*)

scattered than those of GPS, BDS, and Galileo, but no explanation for this was given. From our point of view, it is speculated that this phenomenon may be the result of ignoring the GLONASS code IFB. Due to the existence of code IFB, the receiver DCBs of GLONASS for satellites on

different frequency channels are different. If only one receiver DCB parameter is estimated per station, the different parts of receiver DCB for different frequency channels will be presented in the residuals.

For validating our observations, the correlation between the residuals and frequencies needs to be investigated. Shi et al. (2013) found that GLONASS pseudorange IFBs are highly correlated with the receiver firmware version and antenna type. Therefore, the receiver and antenna type of each contributing MGEX station for the period of our experiment will be studied. Approximately 30 different combinations can be observed. A summary of the major combinations that are applied for more than three stations, the corresponding GLONASS observation types, and number of stations is provided in Table 1. Javad and Trimble are the most commonly used receivers at the current MGEX sites, which are capable of tracking all of the GLONASS signals mentioned above. The receivers of Leica and Septentrio, however, are not able to track the GLONASS C1P code observations, and therefore, they will not be discussed further. We select three stations in each of the remaining five groups, where three groups use Javad receivers, and the other two groups use Trimble receivers. The corresponding residuals of the SPRDCBs of three stations from each group on each frequency channel are shown in Fig. 5.

As shown in Fig. 5, the residual distributions of the GLONASS C1C–C1P SPRDCBs slightly differ by frequency channels. The differences are more obvious for GLONASS C1P–C2P SPRDCBs. The residual distributions deviate significantly from zero for the majority of the frequency channels, which indicates the existence of frequency-associated systematic errors. The residuals of the C1P–C2P observations on all of the frequency channels vary from −2 to 2 ns, while the residuals of C1C–C1P are within ±1 ns. It can be clearly observed that the residuals of the C1C–C1P SPRDCBs are relatively more concentrated than those of C1P–C2P SPRDCB. It can also be seen that the trend of residuals over frequency channels at one station is similar for other stations in the same group with the same receiver and antenna type (shown in each row), while the trends are different for different groups (e.g., in each column). These findings indicate that the residuals of the GLONASS SPRDCBs are closely related to the frequency, which again may be caused by the ignored GLONASS code IFB.

Analysis of the DCB estimation results with GLONASS code IFB consideration

In order to obtain GLONASS DCB products with higher accuracy, we estimate the DCB with GLONASS code IFB consideration. A receiver DCB parameter per frequency channel at a station is estimated using (9). All of the residuals are presented in Fig. 6, which shows that the residuals of the C1C–C1P and C1P–C2P SPRDCBs are close to a normal distribution, with STDs of 0.04 and 0.15 ns, respectively. The residuals are much smaller than those of the corresponding GLONASS SPRDCBs residuals shown in Fig. 4, while they are similar to those of GPS C1C–C1W and C1W–C2W SPRDCB.

The residuals of the selected stations are also plotted in Fig. 7. The residuals on each frequency channel exhibit a characteristic mean of zero, and the frequency-dependent trends shown in Fig. 5 also disappear. The residuals of the C1P–C2P SPRDCBs are also more scattered than those of the C1C–C1P SPRDCBs. The divergence of the residuals on each frequency channel varies, but the largest range is within 1 ns. Moreover, the residuals are independent of the receiver and antenna types, which indicate that the systematic errors of the residuals will be eliminated in DCB estimation when the GLONASS code IFB is considered.

The systematic errors shown in Fig. 5 can be eliminated by considering the GLONASS code IFB. However, to what extent the DCB estimation will be affected by the GLONASS code IFB is still unclear. Since the IFDCB is defined as the difference of DCB estimation with and without consideration of the GLONASS code IFB, it can be used to reflect the influence of the GLONASS code IFB on DCB

Table 1 Receiver and Antenna types used to analyze the GLONASS code IFB. Observations types are based on RINEX 3 observation codes (IGS 2013)

Receiver type	Antenna type	GLONASS observations	Sites	Group
JAVAD TRE_G3TH DELTA	JAV_RINGANT_G3T	1C, 1P, 2P, 2C	17	a
	LEIAR25.R3	1C, 1P, 2P, 2C	5	b
	TRM57971.00	1C, 1P, 2P, 2C	3	c
SEPT POLARX4	LEIAR25.R4	1C, 2P, 2C	3	–
	SEPCHOKE_MC	1C, 2P, 2C	6	–
LEICA GR10/GR25	LEIAR25.R4	1C, 2P, 2C	3	–
	LEIAR25.R4	1C, 2P, 2C	7	–
TRIMBLE NETR9	TRM57971.00	1C, 1P, 2P, 2C	6	d
	TRM59800.00	1C, 1P, 2P, 2C	38	e

Fig. 5 Residuals of GLONASS C1C–C1P and C1P–C2P SPRDCBs obtained by DCB estimation without GLONASS code IFB consideration are plotted for each frequency channel for the selected sites. *Blue* and *red dots* denote the residuals of the C1C–C1P and C1P–C2P SPRDCBs, respectively
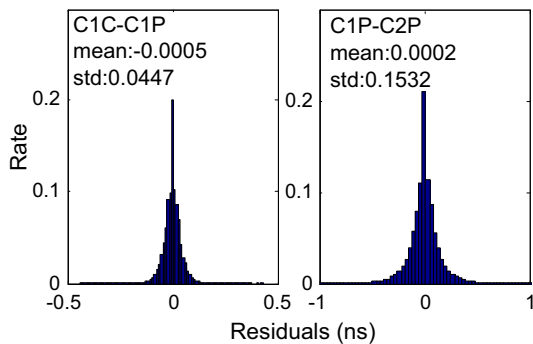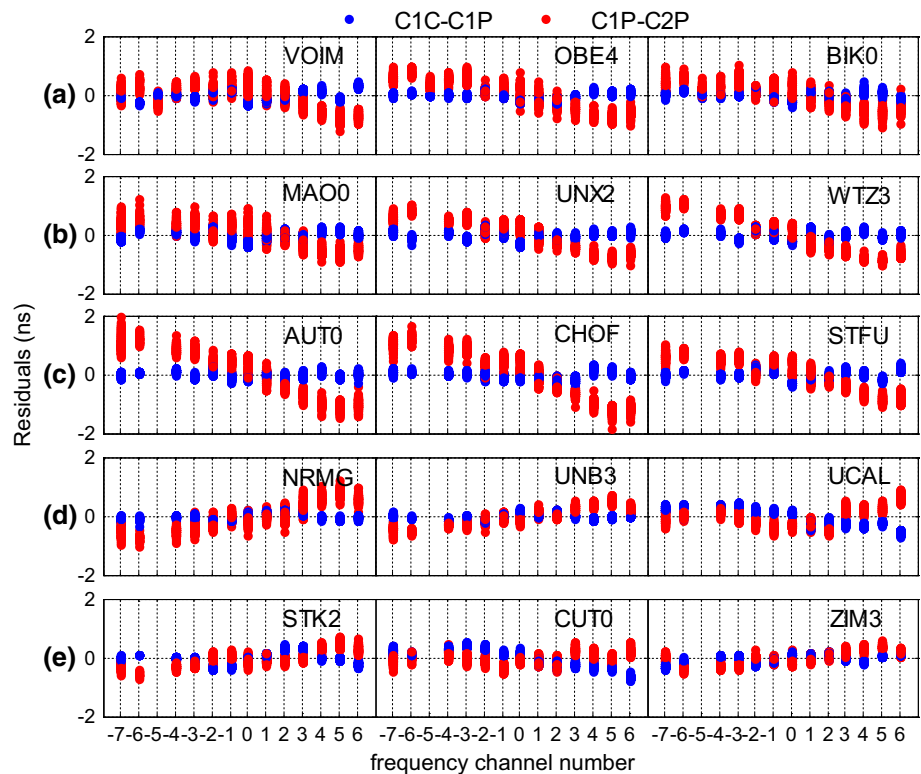
Fig. 6 Residual distributions of the GLONASS C1C–C1P and C1P–C2P SPRDCBs, which are obtained by DCB estimation with GLONASS code IFB consideration, overlaid with normal probability density function curves (*in red*)

estimation. The IFDCBs of the selected sites on DOY 50 in 2016 are illustrated in Fig. 8. It can be seen that the range of C1P–C2P IFDCBs is larger than that of C1C–C1P. The IFDCBs of C1P–C2P are mainly within ±4 ns, in comparison with ±2 ns in the case of the C1C–C1P. The IFDCBs of C1P–C2P and C1C–C1P are different for different frequency channels at each station. The largest difference of C1P–C2P IFDCBs between frequency channels is more than 7 ns and that of C1C–C1P IFDCBs is approximately 4 ns. This analysis indicates that the influence of the GLONASS code IFB on DCB estimation can be as much as several nanoseconds.

Analysis of the influence of the GLONASS code IFB on ionospheric modeling

In order to analyze the effect of the GLONASS code IFB on GPS/GLONASS combined ionospheric modeling, we estimate the VTEC with and without GLONASS code IFB consideration based on data from the MGEX and IGS networks for 30 days (DOY 1–30, 2016). The estimated VTECs are compared with the IGS products. The differences between the two solutions at UTC 6:00 for DOY 10 in 2016 are shown in Fig. 9. It is observed that the estimated VTECs agree well with the IGS data, with the differences being <2 TECU in most areas. It is noteworthy that the accuracy of the IGS GIM products ranges from 2 to 8 TECU, which indicates that the estimated VTEC products are reliable.

In order to distinguish the differences between VTEC products with and without GLONASS code IFB consideration, Fig. 10 shows the differences of VTEC products obtained from ionospheric modeling with and without GLONASS code IFB consideration at UTC 6:00 for DOY 10 in 2016. One can see that the difference between the two solutions is very small, that it exceeds 2 TECU only for several sites, with the largest difference being <4 TECU.

The statistical VTEC differences between ionospheric modeling with and without GLONASS code IFB consideration during DOY 1–30 in 2016 are presented in Fig. 11. The results show that the mean differences of the VTEC

Fig. 7 Residuals of the GLONASS C1C–C1P and C1P–C2P SPRDCBs obtained by DCB estimation with GLONASS code IFB consideration on each frequency channel for the selected sites. *Blue* and *red dots* denote the residuals of the C1C–C1P and C1P–C2P SPRDCBs, respectively
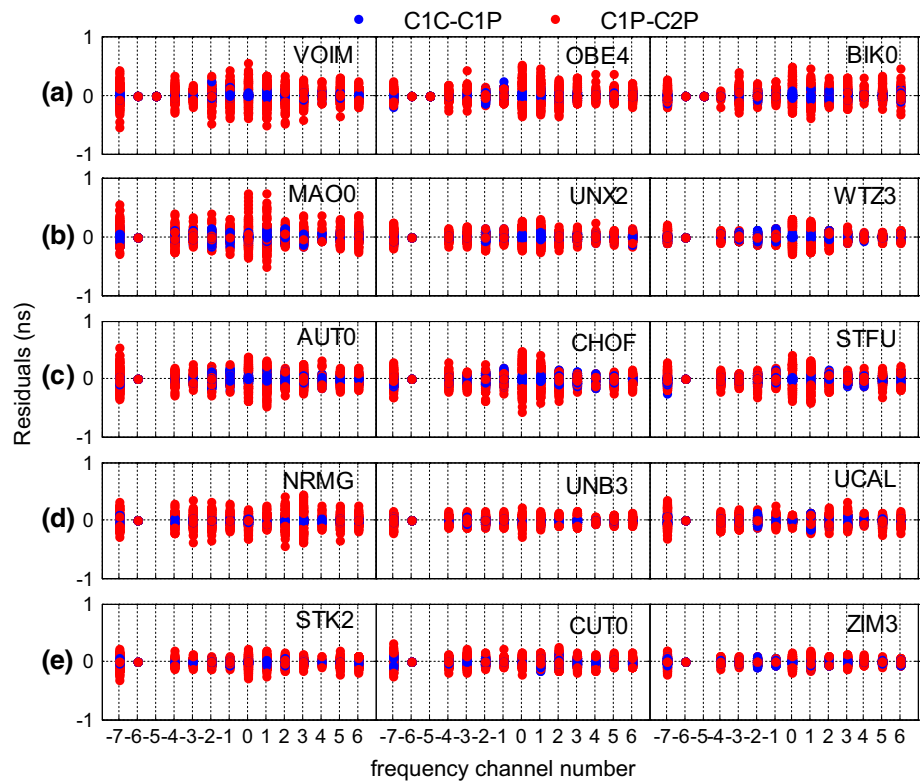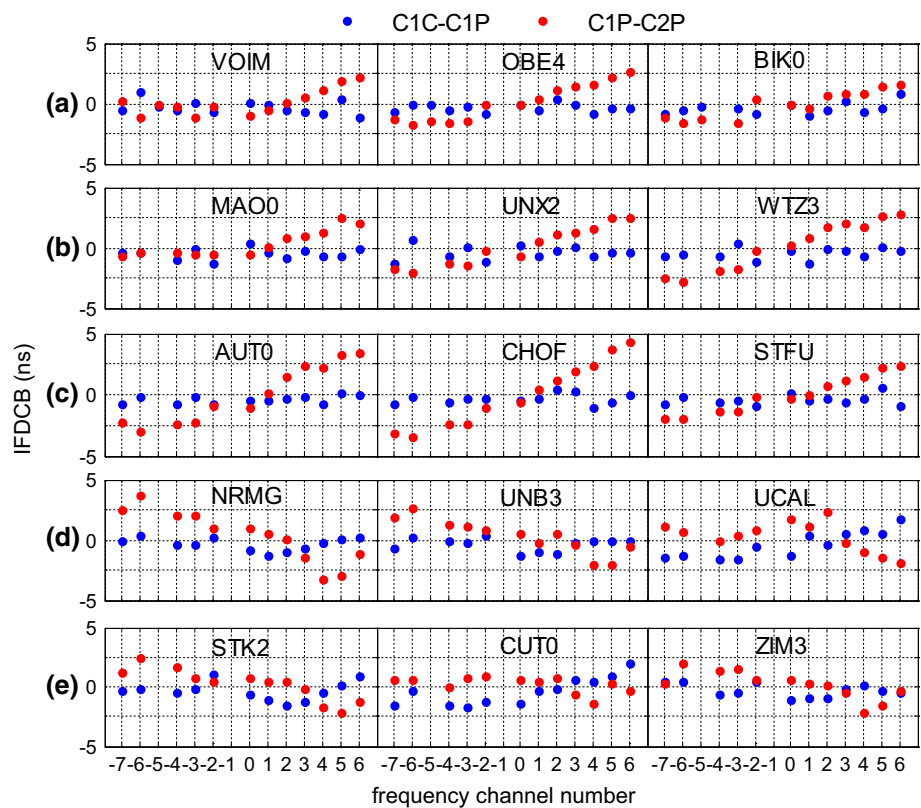

Fig. 8 GLONASS C1C–C1P and C1P–C2P IFDCBs on DOY 50, 2016 at some selected sites. *Blue* and *red dots* denote C1C–C1P and C1P–C2P IFDCBs, respectively
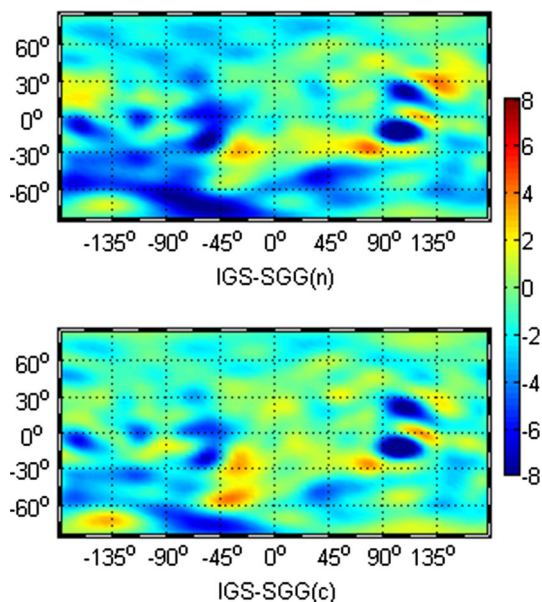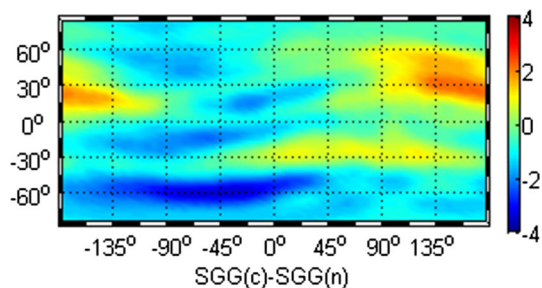
Fig. 9 Differences between VTEC products obtained from ionospheric modeling with (*top*) and without (*bottom*) GLONASS code IFB consideration with respect to IGS at UTC 6:00 for DOY 10, 2016
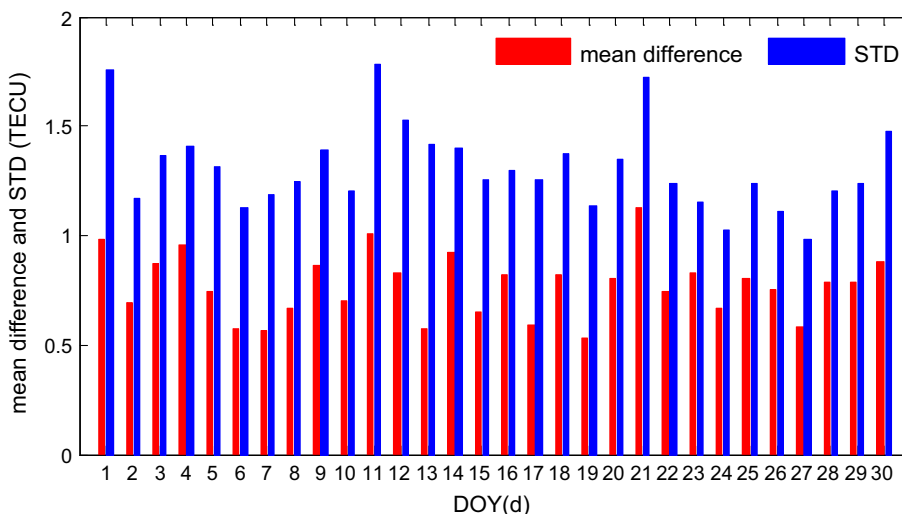

Fig. 10 Differences of VTEC products between ionospheric modeling with and without GLONASS code IFB consideration at UTC 6:00 for DOY 10, 2016

vary between 0.53 and 1.13 TECU. The STD is slightly larger than the mean difference, ranging from 0.98 to 1.75 TECU. As the mean difference and STD of VTEC products with and without GLONASS code IFB consideration are much smaller than the accuracy of the current GIM products, which is in the range of 2–8 TECU, ignoring the GLONASS code IFB shows only a slight effect on the GPS/GLONASS combined ionospheric modeling at present. However, the effect of the GLONASS code IFB might be more pronounced in the future, when the accuracy of ionospheric modeling is improved.

Summary and conclusion

In this study, we investigated the influence of the GLO-NASS code IFB on DCB estimation and GPS/GLONASS combined ionospheric modeling. To evaluate the effect of GLONASS code IFB on DCB estimation, observations from more than 130 MGEX stations were used. First, the DCB products of GPS and GLONASS were generated without considering GLONASS code IFB, which were compared and validated with the DCB products provided by CODE, DLR, and IGG. Then, the residuals from the DCB estimation were analyzed. It was found that the residuals of the GLONASS SPRDCB estimation are much more scattered than those of GPS and that the former exhibit frequency-dependent systematic errors. Afterward, the GLONASS DCBs with code IFB consideration were also estimated. The results show that the STDs of the residuals are much smaller than those of DCB estimation without considering the GLONASS code IFB, and the systematic errors are also eliminated. The IFDCBs of C1P–C2P mainly vary from −4 to 4 ns, and the largest difference between IFDCBs for different channels is more than

Fig. 11 Mean difference and STD of the GIM products between ionospheric modeling with and without GLONASS code IFB consideration from DOY 1 to 30 in 2016. The *red bars* denote the mean difference of VTEC, and the *blue bars* denote the STD

7 ns. In comparison, the IFDCBs of C1C–C1P are slightly smaller, within ± 2 ns. These results indicate that the influence of the GLONASS code IFB on DCB estimation can be as much as several nanoseconds.

The difference of VTEC products obtained from GPS/GLONASS combined ionospheric modeling with and without GLONASS code IFB consideration was also evaluated using data from MGEX and IGS networks for DOY 1–30 in 2016. We found that the mean difference and STD approximately ranged from 0.53 to 1.13 and 0.98 to 1.75 TECU, respectively. Since these mean differences and STD of VTEC products are much smaller than the accuracy of the current GIM products, ignoring the GLONASS code IFB shows no obvious harmful effect on the GPS/GLONASS combined ionospheric modeling at present. However, it is noteworthy that the effect of the GLONASS code IFB might not be so easily ignorable when the accuracy of ionospheric modeling improves in the future.

References

Al-Shaery A, Zhang S, Rizos C (2013) An enhanced calibration method of GLONASS inter-channel bias for GNSS RTK. GPS Solut 17(2):165–173

Ciraolo L, Azpilicueta F, Brunini C, Meza A, Radicella SM (2007) Calibration errors on experimental slant total electron content (TEC) determined with GPS. J Geod 81(2):111–120

Conte JF, Azpilicueta F, Brunini C (2011) Accuracy assessment of the GPS-TEC calibration constants by means of a simulation technique. J Geod 85(10):707–714

Feltens J (2003) The activities of the ionosphere working group of the international GPS service (IGS). GPS Solut 7(1):41–46

Feltens J (2007) Development of a new three-dimensional mathematical ionosphere model at European Space Agency/European Space Operations Centre. Space Weather 5(12):S12002

Hauschild A, Montenbruck O (2016) A study on the dependency of GNSS pseudorange biases on correlator spacing. GPS Solut 20(2):159–171

Hernández-Pajares M, Juan JM, Sanz J (1999) New approaches in global ionospheric determination using ground GPS data. J Atmos Sol Terr Phys 61(16):1237–1247

Hernández-Pajares M, Juan JM, Sanz J, Orus R, Garcia-Rigo A, Feltens J, Komjathy A, Schaer SC, Krankowski A (2009) The IGS VTEC maps: a reliable source of ionospheric information since 1998. J Geod 83(3–4):263–275

ICD-GLONASS (2008) Global navigation satellite system GLONASS interface control document, version 5.1, Moscow

IGS (2013) "RINEX—the receiver independent exchange format"; Version 3.02; IGS RINEX WG and RTCM-SC104

Kozlov D, Tkachenko M, Tochilin A (2000) Statistical characterization of hardware biases in GPS + GLONASS receivers. In: Proc. ION GPS 2000, Institution of Navigation, Salt Lake City, UT, USA, 19–22 Sept, pp 817–826

Lanyi GE, Roth T (1988) A comparison of mapped and measured total ionospheric electron content using global positioning system and beacon satellite observations. Radio Sci 23(4):483–492

Li Z, Yuan Y, Li H, Ou J, Huo X (2012) Two-step method for the determination of the differential code biases of COMPASS satellites. J Geod 86(11):1059–1076

Li X, Ge M, Zhang H, Wickert J (2013) A method for improving uncalibrated phase delay estimation and ambiguity-fixing in real-time precise point positioning. J Geod 87(5):405–416

Li Z, Yuan Y, Wang N, Hernández-Pajares M, Huo X (2015) SHPTS: towards a new method for generating precise global ionospheric TEC map based on spherical harmonic and generalized trigonometric series functions. J Geod 89(4):331–345

Mannucci AJ, Wilson BD, Yuan DN, Ho CH, Lindqwister UJ, Runge TF (1998) A global mapping technique for GPS-derived ionospheric total electron content measurements. Radio Sci 33(3):565–582

Montenbruck O, Hauschild A, Steigenberger P (2014) Differential code bias estimation using multi-GNSS observations and global ionosphere maps. Navigation 61(3):191–201

Øvstedal O (2002) Absolute positioning with single frequency GPS receivers. GPS Solut 5(4):33–44

Pratt M, Burke B, Misra P (1998) Single-epoch integer ambiguity resolution with GPS-GLONASS L1–L2 data. In: Proceedings of the (ION GPS 98), Institute of Navigation, Nashville, TN, 15–18 Sept, pp 389–398

Ren X, Zhang X, Xie W, Zhang K, Yuan Y, Li X (2016) Global ionospheric modelling using multi-GNSS: BeiDou, Galileo, GLONASS and GPS. Sci Rep 6:33499

Schaer S (1999) Mapping and predicting the earth's ionosphere using the global positioning system. Ph.d. dissertation, The University of Bern, Bern

Shi C, Yi W, Song W, Lou Y, Yao Y, Zhang R (2013) GLONASS pseudorange inter-channel biases and their effects on combined GPS/GLONASS precise point positioning. GPS Solut 17(4):439–451

Tsujii T, Harigae M, Inagaki T (2000) Flight tests of GPS/GLONASS precise positioning versus dual frequency KGPS profile. Earth Planet Space 52:825–829

Wang N, Yuan Y, Li Z, Montenbruck O, Tan B (2015) Determination of differential code biases with multi-GNSS observations. J Geod 90(3):209–228

Wanninger L (2012) Carrier phase inter-frequency biases of GLONASS receivers. J Geod 86(2):139–148

Wielgosz P (2011) Quality assessment of GPS rapid static positioning with weighted ionospheric parameters in generalized least squares. GPS Solut 15(2):89–99

Wilson BD, Mannucci AJ (1993) Instrumental biases in ionospheric measurements derived from gps data. In: Proc. ION GPS 1993, Salt Lake City, UT, USA, 22–24 Sept, pp 1343–1351

Yamada H, Takasu T, Kubo N, Yasuda A (2010) Evaluation and calibration of receiver inter-channel biases for RTK-GPS/GLONASS. In: 23rd international technical meeting of the satellite division of the institute of navigation, Portland, 21–24 Sept, pp 1580–1587
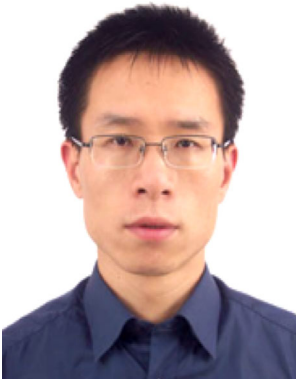
Dr. Xiaohong Zhang is currently a professor at the Wuhan University. He obtained his B.Sc., Master, and Ph.D. degrees with distinction in Geodesy and Engineering Surveying at the School of Geodesy and Geomatics in Wuhan University in 1997, 1999, and 2002. His main research interests include Precise Point Positioning and GNSS/INS.

Dr. Xingxing Li is currently a scientist at GFZ. He has completed his B.Sc. degree at the school of Geodesy and Geomatics in Wuhan University. He obtained his Ph.D. degrees at the Department of Geodesy and Remote Sensing of the German Research Centre for Geosciences (GFZ). His current research mainly involves GNSS precise data processing and its application for geosciences.

Weiliang Xie is currently a Master candidate at the Wuhan University. He has completed his B.Sc. at the School of Earth Science and environmental engineering in Southwest Jiao Tong University. His area of research currently focuses on the ionospheric modeling and the estimation and characteristics of multi-GNSS differential code bias.

Keke Zhang is currently a Master candidate at the Wuhan University. He has completed his B.Sc. at the School of Geodesy and Geomatics in Wuhan University. His area of research currently focuses on the GNSS precise data processing and ionospheric modeling.

Xiaodong Ren is currently a Ph.D. candidate at the Wuhan University. He obtained his B.Sc. and Master degrees with distinction in Geodesy and Engineering Surveying at the School of Geodesy and Geomatics in Wuhan University in 2007 and 2011. His main research focuses on PPP-RTK and ionosphere modeling.

Dr. Weiping Jiang is currently a professor at the Wuhan University. He obtained his B.Sc., Master, and Ph.D. degrees with distinction in Geodesy and Engineering Surveying at the School of Geodesy and Geomatics in Wuhan University in 1995, 1997, and 2001. His main research interests include GNSS data processing and satellite gravity.